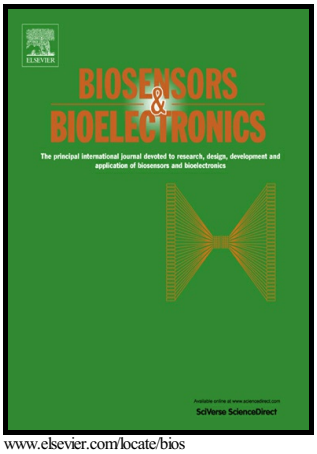

www.elsevier.com/locate/bios

Direct detection of two different tumor-derived extracellular vesicles by SAM-AuNIs LSPR biosensor

Abhimanyu Thakur, Guangyu Qiu, Siu-Pang NG, Jintao Guan, Jianbo Yue, Youngjin Lee, Chi-Man Lawrence Wu

PII: S0956-5663(17)30187-2
DOI: http://dx.doi.org/10.1016/j.bios.2017.03.036
Reference: BIOS9624

To appear in: *Biosensors and Bioelectronic*

Received date: 7 December 2016
Revised date: 1 March 2017
Accepted date: 16 March 2017

Cite this article as: Abhimanyu Thakur, Guangyu Qiu, Siu-Pang NG, Jintao Guan, Jianbo Yue, Youngjin Lee and Chi-Man Lawrence Wu, Direct detection of two different tumor-derived extracellular vesicles by SAM-AuNIs LSPR biosensor, *Biosensors and Bioelectronic* http://dx.doi.org/10.1016/j.bios.2017.03.036

Direct detection of two different tumor-derived extracellular vesicles by SAM-AuNIs LSPR biosensor

Abhimanyu Thakur[a1], Guangyu Qiu[b1], Siu-Pang NG[b], Jintao Guan[a], Jianbo Yue[a], Youngjin Lee[a*], Chi-Man Lawrence Wu[b*]

[a]Department of Biomedical Sciences, City University of Hong Kong, Hong Kong SAR, Hong Kong,
[b]Department of Physics and Materials Science, City University of Hong Kong, Hong Kong SAR, Hong Kong

[*]Corresponding authors: Youngjin Lee & Chi Man Lawrence Wu

Youngjin Lee, Department of Biomedical Sciences, City University of Hong Kong, 83 Tat Chee Avenue, Kowloon, Hong Kong SAR, Hong Kong, Tel.: +852-3442-4313, E-mail: younglee@cityu.edu.hk

Chi Man Lawrence Wu, Department of Physics and Materials Science, City University of Hong Kong, 83 Tat Chee Avenue, Kowloon, Hong Kong SAR, Hong Kong, Tel.: +852-3442-8668, E-mail: lawrence.wu@cityu.edu.hk

Abstract
Extracellular vesicles (EVs) are abundant in various biological fluids including blood, saliva, urine, as well as extracellular milieu. Accumulating evidence has indicated that EVs, which contain functional proteins and small RNAs, facilitate intercellular communication between neighbouring cells, and are critical to maintain various physiological processes. In contrast, EV-derived toxic signals can spread out over the tissues adjacent to the injured area in certain diseases, including brain tumors and neurodegenerative disorders. This demands better characterization of EVs which can be employed for liquid biopsy clinically as well as for the study of intercellular signalling. Exosomes and microvesicles share a number of similar characteristics, but it is important to distinguish between these two types of EVs. Here, we report for the first time that our in-house developed Localized Surface Plasmon Resonance biosensor with self-assembly gold nanoislands (SAM-AuNIs) can be used to detect and distinguish exosomes from MVs isolated from A-549 cells, SH-SY5Y cells, blood serum, and urine from a lung cancer mouse model. Exosomes, compared with MVs, produced a distinguishable response to the bare LSPR biosensor without functionalization, suggesting a different biophysical interaction between exosomes and MVs with SAM AuNIs. This sensor attains the limit of detection to 0.194 µg/ml, and the linear dynamic range covers 0.194-100 µg/ml. This discovery not only reveals great insight into the distinctive membrane property of tumor-derived exosomes and MVs, but also facilitate the development of novel LSPR biosensors for direct detection and isolation of heterogeneous EVs.

Keywords
Biosensor, Exosome, Microvesicles, Extracellular Vesicles, LSPR, Tumor Prognosis.

[1] These authors contributed equally to this work

1. Introduction

Extracellular vesicles (EVs), known as microparticles, shedding vesicles, or oncosomes (György et al., 2011), are released from a wide range of cells, including tumor cells. Accumulating evidence has indicated that EVs, which contain a number of proteins and small RNAs, can influence the function of recipient cells (Yáñez-Mó et al., 2015). Tumor-derived exosomes can spread out over the tissues adjacent to the injured area of certain diseases, including brain tumors and neurodegenerative disorders (Gangoda, Lahiru, et al, 2015). In general, EVs consist of exosomes, microvesicles, apoptotic bodies, etc. They have long been recognized as heterogeneous vesicles in their size and surface proteins depending on their biogenesis in the parental cells. However, biophysical heterogeneity of EVs has not been clearly investigated so far.

Exosomes are cell-derived EVs that are present in perhaps all biological fluids including urine, blood, cerebrospinal fluid, fractions of body fluids such as serum, plasma, and cell cultured medium (Li et al., 2014, Lin et al., 2015, van der Pol et al., 2012, Pocsfalvi et al., 2016). The diameter of exosomes ranges from 30 to 100 nm and their morphology is cup-shaped as described through analysis using transmission electron microscopy (TEM). Exosomes are characterized by the presence of proteins involved in membrane transport and vesicular fusion, by components of the endosomal sorting complex required for transport (ESCRT) complex, and by tetraspanins, such as CD9 and CD63, on their membrane (Chaput et al., 2011). Compared with exosomes, multivesicular vesicles (MVs) are budded directly from the plasma membrane, and are released into most of the biological fluids, including conditioned culture medium (Beyer et al., 2010, Morel et al., 2011). Although MVs are believed to be larger than exosomes and usually range in size from 100 nm to 1.0 μm in diameter (Théry et al., 2009), there is much uncertainty on this aspect.

The important criteria to differentiate the types of extracellular vesicles are size and morphology (Gould et al., 2003). In general, determining the size of vesicles is based on TEM analysis (Van Der Pol et al., 2010); visualization by negative staining TEM is one of the ways to identify exosomes through detecting their cup-shaped morphology and size (Marzesco et al., 2005), while other methods to directly determine the size and concentration of vesicles in suspension include atomic force microscopy (Yuana et al., 2010) and nanoparticle tracking analysis (Marzesco et al., 2005).

For a long time surface plasmon resonance (SPR) biosensing has been a well-known sensitive method to detect various biomaterials such as DNA (Tamada et al., 2007, Sikarwar et al., 2017), RNA (Florschütz et al., 2013, Amano et al., 2016), protein (Huang et al., 2007, Canoa et al., 2017) and peptides (Soler et al., 2016). Interestingly, many SPR-based methods have also been developed to detect EVs, including exosomes and MVs (Supplementary-Table S1). In the detection of EVs with an SPR biosensor, immunolabeling has been used to functionalize the SPR surface with an EV-specific antibody, which is a time-consuming process and involves additional chemicals.

LSPR results from the confinement of a strong electromagnetic field exhibited by a noble metal in its nanostructural form. Nano size gold structures have shown higher sensitivity to local refractive index variation adjacent to the gold nanosurface. LSPR nanostructures are further classified into two different categories: (i) regular nanopatterns and (ii) random distributed nanostructures. The regular patterns, such as nanoholes, nanopillars, and nanodisks, are synthesized by electron beam lithographic techniques or mask-assist

techniques, which require complex processes of the synthesis and entail high costs. Particularly, randomly distributed gold nanoislands were well studied and substantially reduced the cost of LSPR sensing systems. Random arrays of self-assembly gold nanoislands (SAM-AuNIs) were fabricated by a two-step deposition-annealing process. This method provides a convenient way to mass-produce sensitive and low-cost optochemical biosensors. Therefore, in detecting EVs, we utilized our previously reported SAM-AuNIs LSPR biosensing system (Qiu et al., 2016, Ng et al., 2016). Due to the localized plasmonic resonance effect, the linear polarized transverse magnetic (TM) light shows significant transition in phase after total internal reflection on the metal-dielectric interface, and the phase transition only appears at the extinction wavelength on refractive index variation.

In this work, we employed the spectral phase detection LSPR interferometer, a highly sensitive optical biosensing technique, to distinguish exosomes from MVs. We discovered for the first time that the two different tumor-derived EVs; exosomes and MVs, can be distinguished using bared SAM-AuNIs LSPR without functionalization with an antibody.

2. Materials and Methods

2.1. Ethics statements

Animal experimental protocols were approved by the Animal Research Ethics Sub-Committee in City University of Hong Kong and Department of Health, Government of the Hong Kong Special Administrative Region.

2.2 Cell Culture

Human lung cancer A549 cells (gift from Professor Mingshu Yang, City University of Hong Kong) were maintained in Dulbeco's modified essential medium (DMEM) (Life Technologies) supplemented with 10% FBS at 37°C and under 5% CO_2.

Human neuroblastoma SH-SY5Y cells (gift from Dr. Mingliang He, City University of Hong Kong) were maintained in a mixture of Eagle's Minimum Essential Medium (EMEM) and F-12 Medium (1:1 ratio) supplemented with 10% FBS at 37°C and under 5% CO_2.

Both the cell types were grown to 70% confluency, washed 3 times with PBS and incubated for 24 hours in serum free media.

2.3. Isolation of exosomes and microvesicles from cells

Exosomes from both A-549 and SH-SY5Y cells were isolated using a previously published protocol (Xu et al., 2015) with slight modification (Supplementary-figure S1A). In brief, after obtaining conditioned medium from the culture, it was centrifuged at 300 ×g for 10 minutes. The resultant supernatant was further centrifuged at 16,500 ×g for 20 minutes followed by filtration of successive supernatant through 0.2 μm filter (to remove apoptotic bodies and microvesicles). The resultant supernatant was ultra-centrifuged at 120,000 ×g for 70 minutes to extract exosomes.

Isolation of microvesicles was performed using a previously published protocol (Li et al., 2014) with slight modification (Supplementary-figure S1A). In brief, the conditioned medium from the culture was centrifuged at 300 ×g for 10 minutes. The resultant supernatant was further centrifuged at 2,000 ×g for 20 minutes followed by filtration of successive supernatant through 0.8 μm filter (to remove apoptotic bodies). Then, the resultant supernatant was centrifuged at 12,200 ×g for 40 minutes to extract microvesicles.

2.4. Blood serum preparation

Blood serum was prepared according to a previously published protocol (Almqvist et al., 2008). In brief, the blood from mice was obtained by cardiac puncture and stored in an EDTA tube. To obtain the serum the blood was centrifuged twice at 3,000 ×g for 10 min at room temperature.

2.5. Isolation of exosomes and microvesicles from mouse blood and urine

From mouse blood serum, exosomes were isolated by using Total exosome isolation (from serum) reagent (Invitrogen) as per manufacturer's instruction (Li et al., 2014). Microvesicles were isolated from blood as per previously published method (Jayachandran et al., 2012) as shown in supplementary-figure S1B. Exosomes were isolated from mouse urine by using Exoquick solution (System Bioscience, Cat# EXOTC10A-1), and MVs were isolated as described previously (Rood et al., 2010).

2.6. Transmission Electron Microscopy (TEM)

The morphology and particle size of exosomes and microvesicles dissolved in PBS were characterized by using TEM according to a previously published protocol with slight modification (Théry et al., 2006).

2.7. Size distribution and zeta potential analysis

Size distribution of exosomes and MVs were analyzed by using Malvern NanoSight NS300 as described previously (Mazzeo et al., 2015). Zeta potential of exosomes and MVs were analyzed by Malvern Zetasizer Nano ZS.

2.8. Immunogold Electron Microscopy

Immunogold-EM analysis of vesicles was performed as described previously (Kesimer et al., 2009). Briefly, for the immuno-gold labeling with antibodies, blocked grids were transferred to a drop of the antibody (anti-CD9 for exosomes and anti-integrin for MVs) in PBS/0.5% BSA and incubated for 30 min. The grids were then washed with PBS/0.5% BSA 5 times for 3 min, incubated with gold-labelled secondary antibody in PBS/0.5% BSA for 30 min, and then washed 5 times for 3 min in 100 µl drops of PBS/0.5% BSA. The grids were stained with 2% uranyl acetate and then viewed under Transmission Electron Microscope (FEI/ Philips Tecnai 12 BioTWIN).

2.9. Fabrication of SAM-AuNIs localized surface plasmon resonance (LSPR) spectroscopy

The synthesis of SAM-AuNIs sensing chip was introduced in our previous work (Qiu et al., 2015), including the fabrication details and sensing performance optimization. In brief, the SAM-AuNIs sensing chip was fabricated by annealing the as-deposited Au films on a BK7 glass slide. The thickness of deposited Au film was approximately 5.0 nm with 0.79 nm nominal surface roughness. The gold-on-glass thin film was thermally annealed at 550°C for 3 h in air. Tapping mode atomic force microscopy (TM-AFM) was performed and the SAM-AuNIs were found with average diameter of about 40 nm and partially embedded into the BK7 glass substrate.

2.10. Detection of exosomes and MVs with bared SAM-AuNIs chip

The as-synthesised SAM-AuNIs sensing chip (Qiu et al., 2015) was placed into the common-path optical detection system. The phase information, as reported in previous work was extracted from total internal reflected light and calculated by windows fourier transform

(WFT) methods. To analyse the sensitivity of detection of exosomes by LSPR, four different concentrations (1µg/ml, 10 µg/ml, 50 µg/ml and 100µg/ml) of exosomes were injected individually, and the LSPR sensogram was obtained. Subsequently, LSPR response towards exosomes and MVs isolated from A-549 and SH-SY5Y cells were determined. First, 100 µl of 1×PBS was injected into the flow cell to rinse the sensing chip and build the baseline of phase detection. Then, 50 µg/ml exosomes and microvesicles (suspended in PBS) were injected into the probe cell separately and the LSPR sensogram was recorded. The buffer solution was injected again to check the binding affinity between exosomes and AuNIs surface. Any unstable bound particles could be removed by flowing force. The possible interaction between exosomes and SAM-AuNIs is illustrated in schematic figure 2(A). Eventually, LSPR responses towards exosomes and microvesicles isolated from blood serum of lung cancer mouse were also determined in a similar way as described above.

2.11. Force-separation analysis by AFM

The force-strength study was performed with BioScope Catalyst AFM (Bruker). The silicon nitride cantilevers used in the study were calibrated to determine the spring constants to be 0.1974 N/m. Exosomes and MVs were immobilized on the AFM tip (ScanAsyst-Fluid, TELTEC semiconductor pacific limited) after its functionalization as described previously (Sharma et al., 2010). In brief, primary antibodies (anti-CD9 for exosomes and anti-integrin for MVs) were covalently attached to Si_3N_4 AFM probes via thiol ester linkage (Bruker). The probes were washed in PBS, blocked with 1% BSA- PBS for 1 hour followed by rinsing with PBS. Then, exosomes and microvesicles were functionalized. All measurements were recorded in physiological buffer conditions. Adhesion forces between functionalized sensor tips and AuNIs were recorded with single ramping mode. No antibody-coated AFM tips were used as control.

3. Results and Discussions

3.1. Exosomes differ with MVs in terms of morphology and size

Exosomes and MVs were isolated as described by Xu et al., 2015, and Li et al., 2014 respectively. To confirm whether each fraction has exosomes and MVs, TEM analysis was conducted. Exosomes isolated from SH-SY5Y, A-549 cells, and blood serum of lung cancer mouse mostly exhibited circular shape (Figures 1A, 1E, and 1I respectively). Similarly, the MVs isolated from SH-SY5Y, A-549 cells, and blood serum of lung cancer mouse also exhibited round shape (Figures 1B, 1F, and 1J respectively). However, some of the exosomes from SH-SY5Y cells were oval in shape.

Furthermore, the size distribution of all the exosomes and MVs were determined by using Nanosight tracking analyzer NS300. Most of the exosomes isolated from SH-SY5Y, A-549, and blood serum from lung cancer mouse were approximately 63 nm, 73 nm, and 97 nm respectively (Supplementary-figures S2A, S2C, and S2E respectively). These data are within the range of typical exosomal size. In addition, there are some other peaks in all the size distribution curves, which suggests the presence of small amounts of some other EVs as well. Unlike exosomes, the size distribution of all the MVs extends beyond 200 nm. Supplementary-figures S2B, S2D, and S2F show the size distribution of MVs isolated from SH-SY5Y, A-549, and blood serum from lung cancer mouse respectively. For all the MVs, the size distribution range is an overlapping characteristic. Nonetheless, size heterogeneity was constantly observed in both exosomes as well as MVs, demonstrating the presence of a common mechanism to generate various sizes of these vesicles, regardless of parental cells.

In addition, the intensity distribution graphs show that the exosomal fractions derived from SH-SY5Y, A-549, and blood serum from lung cancer mouse are clustered homogeneously within 150 nm (Supplementary-figures S3A, S3C, and S3E respectively). On the contrary, the MVs from SH-SY5Y, A-549, and blood serum from lung cancer mouse are spread over a wide range of size distribution as shown in supplementary-figures S3B, S3D, and S3F respectively.

The isolated exosomes and MVs from SH-SY5Y, A-549, and blood serum from lung cancer mouse were further confirmed by immunogold labeling with an exosomal marker (CD9) (Figures 1C, 1G, 1K), and MV marker (integrin) (Figures 1D, 1H, 1L) repectively. The relative amount of exosomes and MVs isolated from SH-SY5Y, A-549, and blood serum from lung cancer mouse were measured based on protein amount (Supplementary-table S2) by using BCA protein assay, respectively. In general, exosomes were significanly more released than MVs from parental cells. However, the role of differential release of two different types of vesicles from tumor cells remains to be elucidated.

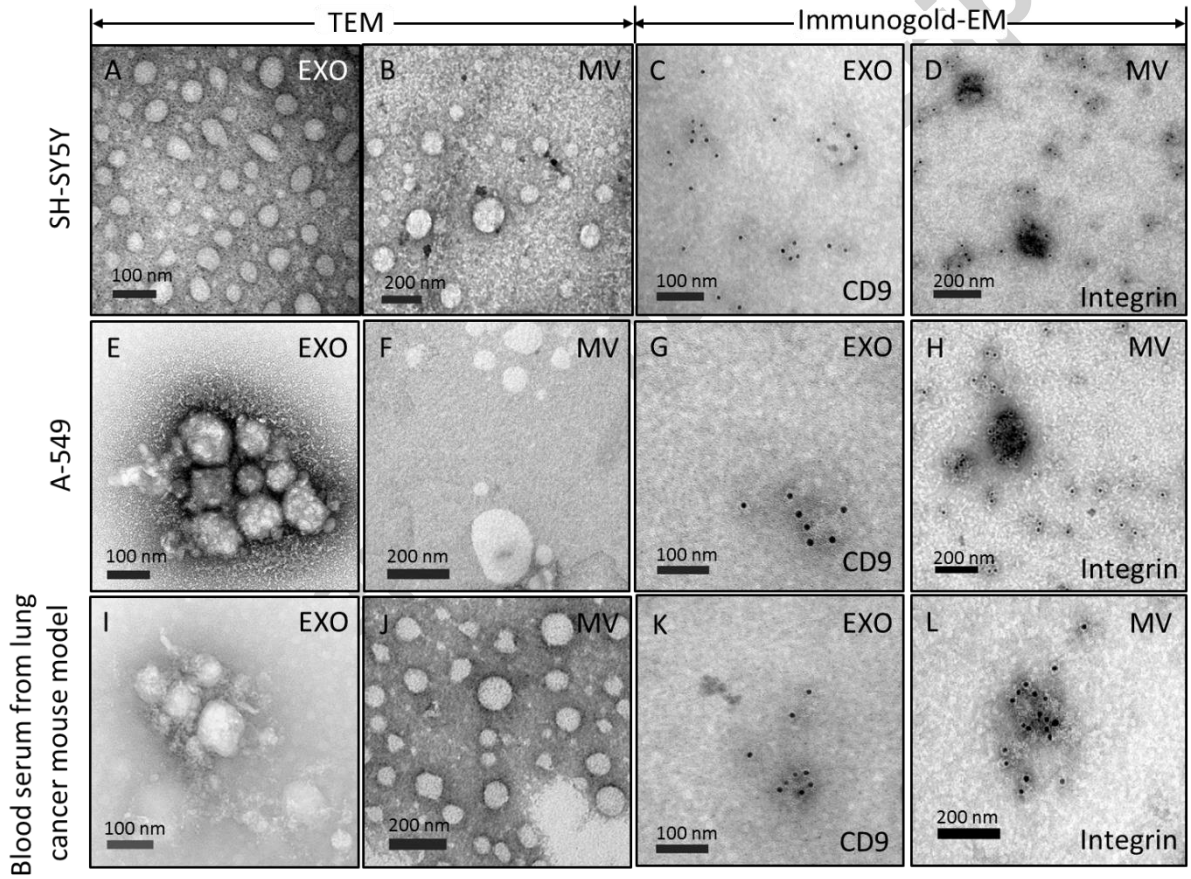

Fig 1 Transmission electron microscopy (TEM) images of exosomes (EXO) isolated from (A) SH-SY5Y, (E) A-549, (I) blood serum of lung cancer mouse (Scale bar: 100 nm). TEM of microvesicles (MVs) isolated from (B) SH-SY5Y, (F) A-549, (J) blood serum of lung cancer mouse (Scale bar: 200 nm). Detection of CD9 on the surface of exosomes isolated from (C) SH-SY5Y, (G) A-549, (K) blood serum of lung cancer mouse model observed by transmission electron microscope (Scale bar: 100 nm). Detection of integrin on MVs isolated

from (D) SH-SY5Y, (H) A-549, (L) blood serum of lung cancer mouse model observed by transmission electron microscope (Scale bar: 200 nm).

3.2. Detection of exosomes on bare SAM-AuNIs chip

Detection of membrane proteins of exosomes and MVs has been performed with an antibody-functionalized LSPR biosensor (Im H et al., 2014). However, it has not been revealed whether exosomes and MVs can be detected distinctively with bare SAM-AuNIs chip LSPR. Interestingly, LSPR response of the surface of bare SAM-AuNIs chip has a strong correlation with the concentration of exosomes derived from A-549 cells (Figure 2C). Figure 2B and supplementary-figure S4 shows the typical real-time phase response of three different concentrations of exosomes derived from A-549 cells (1 µg/ml, 10 µg/ml, and 100 µg/ml based on protein amount). The inset shows the enlarged response of 1 µg/ml exosomes derived from A-549 cells. In this study, the injection of exosomes at 200 s caused the response immediately, and the corresponding value was approximately 0.14 radian. Then, 1× PBS buffer was injected again to rinse the sensing chip and verify the capture of exosomes on bared SAM-AuNIs. A similar strategy was utilized for two succeeding concentrations (10 µg/ml and 100 µg/ml) of exosomes. It indicated that these exosomes were well immobilized onto the SAM-AuNIs and caused the phase response of 0.72 radian and 2.09 radian respectively. Furthermore, 50 µg/ml exosomes solution was also detected with SAM-AuNIs separately as 1.38 radian. Responses of these four concentrations were utilized to calculate the standard curve for detecting exosomes with this SAM-AuNIs LSPR sensor, as shown in figure 2C. The dark point with an error bar stands for the mean response of specific exosomes concentration of A-549 cells with standard deviation of three replicates. The fitted relationship between exosomes concentration (Conc.) and phase response (Res.) is found to be Res. = 0.01793 × Conc. + 0.3641 (R-square = 0.956). Based on this standard curve, the sensitivity of our proposed exosomes SAM-AuNIs sensor was given by the slope at 0.01793 rad/(µg/ml). In addition, the limit of detection (LOD) was determined to be 0.194 µg/ml at triple of its standard deviation (3.12×10^{-3} radian) from blank measurement. The response time is quoted as T90 which is referring to the time taken to achieve 90% of the equilibrium response. The response time T90 of exosomes detection decreased from 1000 seconds to only 400 seconds when the concentration increased from 1 µg/ml to 100 µg/ml. For comparison between antibody functionalized and unfunctionalized SAM-AuNIs LSPR response, experiments were conducted by anti-CD9 and anti-integrin functionalized LSPR as shown in supplementary-figure S5 collectively.

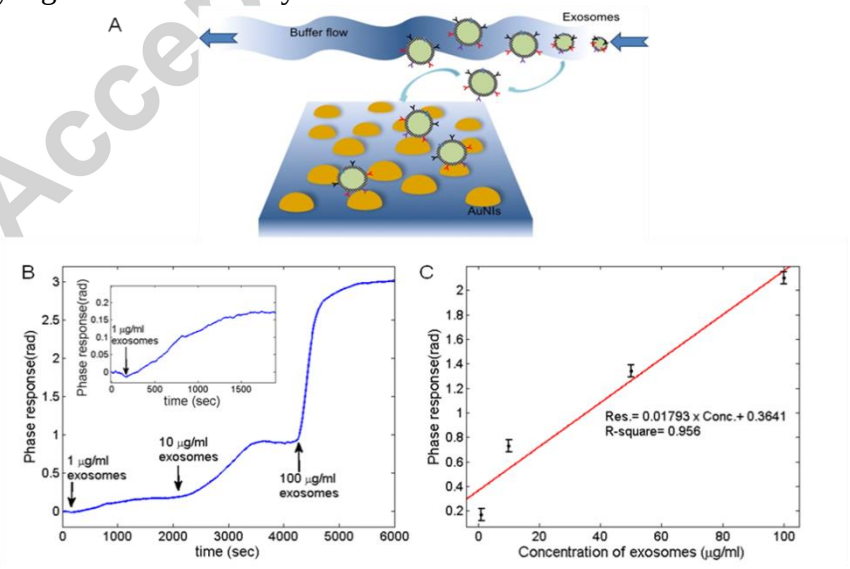

Fig 2 (A) Schematic illustration of the biophysical interaction of exosomes with SAM-AuNIs. (B) Sensitivity of exosome detection by LSPR. LSPR response of three different

concentrations of exosomes (1µg/ml, 10 µg/ml, and 100 µg/ml) was used in the experiment one by one; (C) the maximum phase response was observed for 100 µg/ml.

3.3. LSPR to distinguish between exosomes and microvesicles without an antibody-functionalized SAM-AuNIs

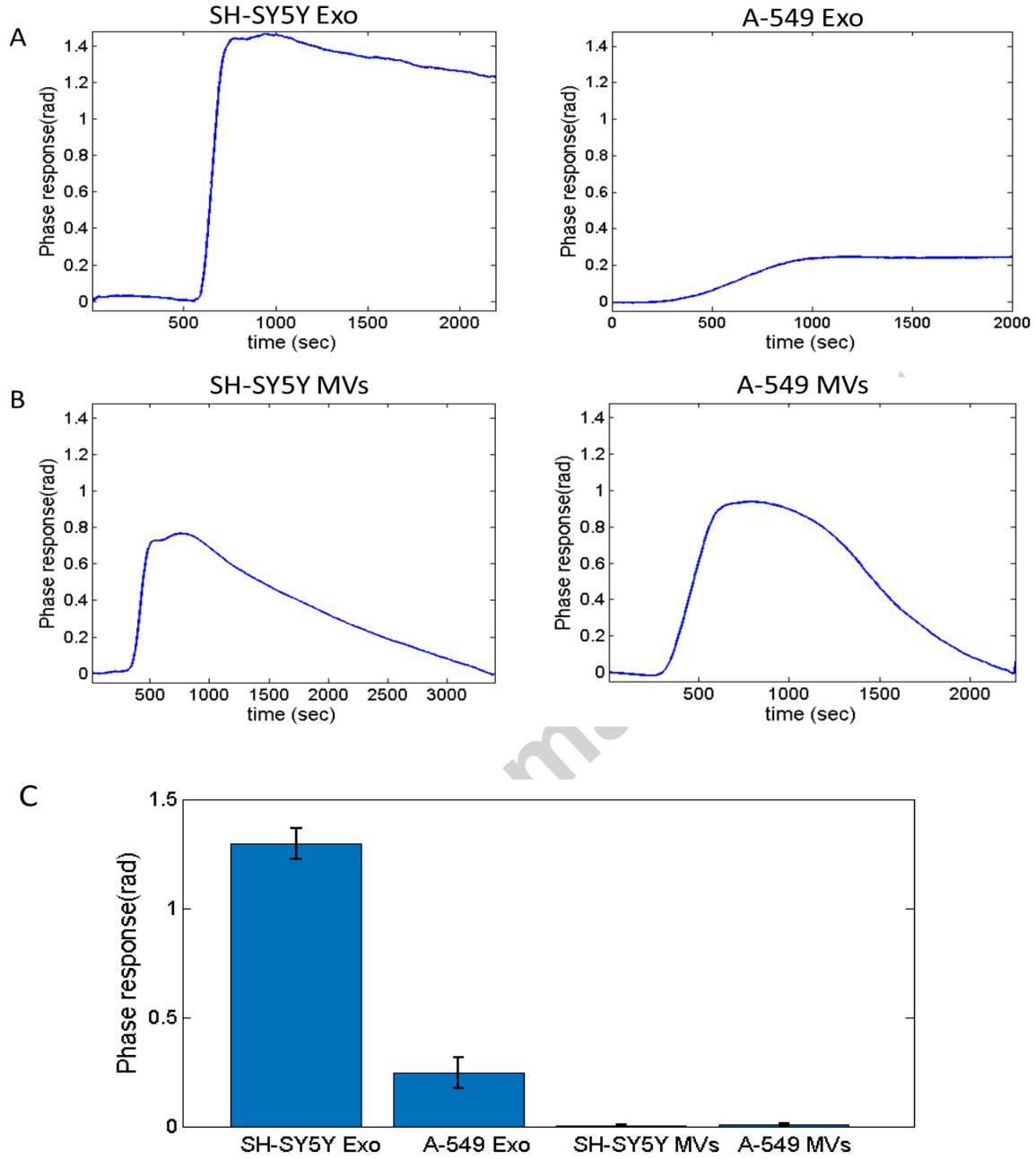

Fig 3 Localized surface plasmon resonance response without any functionalization for exosomes and MVs from both SH-SY5Y and A549 cells. (A) The LSPR phase response for exosomes increased to a maximum value and was maintained at a slightly lower value even after flushing with PBS. (B) The SPR phase response for MVs increased to a maximum value but decreased sharply after flushing with PBS. (C) Bar chart for the maximum phase response for SH-SY5Y exosomes, A-549 exosomes, SH-SY5Y MVs, and A-549 MVs.

An antibody-functionalized LSPR has been progressively developed to detect specfic biomaterials, including EVs. For example, CD9 functionalized LSPR can detect exosomes

specifically (Supplementary-figure S5B and S5C). However, it has not been studied as to whether EVs can directly interact with various LSPR chips.

Interestingly in this work, bare SAM-AuNIs chip without any functionalization could generate LSPR response to exosomes and MVs (data not shown for MVs) in a concentration-dependent manner (Figure 2B), which was similar to the response via an antibody-functionalized SAM-AuNIs LSPR sensor, suggesting the specific biophysical interaction of exosomes and MVs with the chip. Therefore, biophysical detection of the membrane of exosomes and MVs was conducted directly with our antibody-unfunctionalized SAM-AuNIs LSPR sensor. A PBS buffer, pH 7.2 (Cat# 20012050) solution was initially injected into the probe cell to establish the baseline. Then 50 µg/ml exosomes from SH-SY5Y and A-549 cells were injected into the sensing system separately. As shown in figure 3A, exosomes from both cell cultures caused obvious phase responses. For the exosomes from SH-SY5Y cells, the phase response is much higher than that from A-549 exosomes, which indicated that the membrane of SH-SY5Y exosomes is more attracted to bare gold nanoislands. Then the sensing chips were rinsed by PBS buffer (pH 7.2) solution to check the immobility of captured exosomes. For SH-SY5Y exosomes, the phase response slightly decreased but managed to stabilize at above 1.2 radian. For A-549 exosomes, the phase response maintained at about 0.2 radian. In the same manner, the MVs from these two cell cultures were also conducted with new LSPR sensing chips. After the MVs were injected into the probe cell, the phase increased to 0.76 radian and 0.91 radian for SH-SY5Y and A549 cells respectively (Figure 3B). However, after the PBS buffer (pH 7.2) rinse, the phase response value decreased back to the original state. This indicates that the membrane of MVs was not stably attached on bare SAM-AuNIs, unlike that of exososmes. The final phase response values of exosomes and MVs were concluded into the bar chart, with standard deviation of repeated experiments, as shown in Figure 3C. Moreover, similar results were found when the SPR analysis was performed for exosomes and MVs diluted in other buffers, such as tris-buffer saline (TBS) and PBS (pH 7.4) as shown in supplementary figure S6. Thus, the developed SAM-AuNIs sensing system shows higher specificity to exosomes than other EVs based on their different membrane properties. This provides an insight into development of novel LSPR and new purification methods for heterogenous EVs based on this observation. Further, this observation provides an opportunity for studying interaction of biomembranes with various chips (AuNIs, copper, graphene, silver, etc.). In addition, the zeta potential of exosomes and MVs as determined by Malvern Zetasizer Nano ZS (Supplementary figure S7) suggest that exosomes are electrostatically unstable compared to MVs due to more negative zeta potential values for exosomes (Supplementary table S3). This might be reason for exosomes being more attracted to bare gold nanoislands as compared to MVs.

3.4. LSPR response to exosomes and MVs from the blood serum and urine of lung cancer mouse model

Moreover, the specificity of SAM-AuNIs sensor toward exosomes was verified with exosomes and MVs isolated form blood serum of a lung cancer mouse model. The concentration of exosomes and MVs were the same as in previous experiments, i.e. 50 µg/ml. In the initial 500 s, the PBS was injected into the probe cell and the baseline for later detection was built. Then, the mouse blood serum-derived exosomes and MVs were separately injected into the sensing system. Similar to previous results, exosomes were

captured onto the SAM-AuNIs as the phase reading was maintained even after PBS flushing, as shown in figure 4A. Unlike exosomes, the attached MVs were washed away immediately after injection of PBS and the LSPR response returned to the original state (Figure 4B). Furthermore, exosomes and MVs from urine of the lung cancer mouse model also produced a similar pattern of LSPR reponse (Supplementary figure S8).

This illustrates that, although the MVs can also be attracted to the AuNIs, the binding affinity is rather weak. Thus, based on the detection and rinsing process, the SAM-AuNIs LSPR sensing system can easily distinguish exosomes from MVs within 30 minutes. Therefore, our finding provides a clue to develop new LSPR biosensing tools for direct and specific detection of EVs using various chip materials, including copper and graphene. It could also facilitate finding better methods for the efficient isolation of various EVs. In addition, the release and composition of exosomes and MVs from different stages of tumor cells, such as during migration, invasion, or proliferation, might be unique. Therefore, specific values and patterns of direct LSPR response for washout of exosomes and MVs from gold surface could be utilised together with other parameters, including zeta potential and AFM data to monitor the progression of parental tumors. This may be further applicable to cancer diagnosis and prognosis clinically.

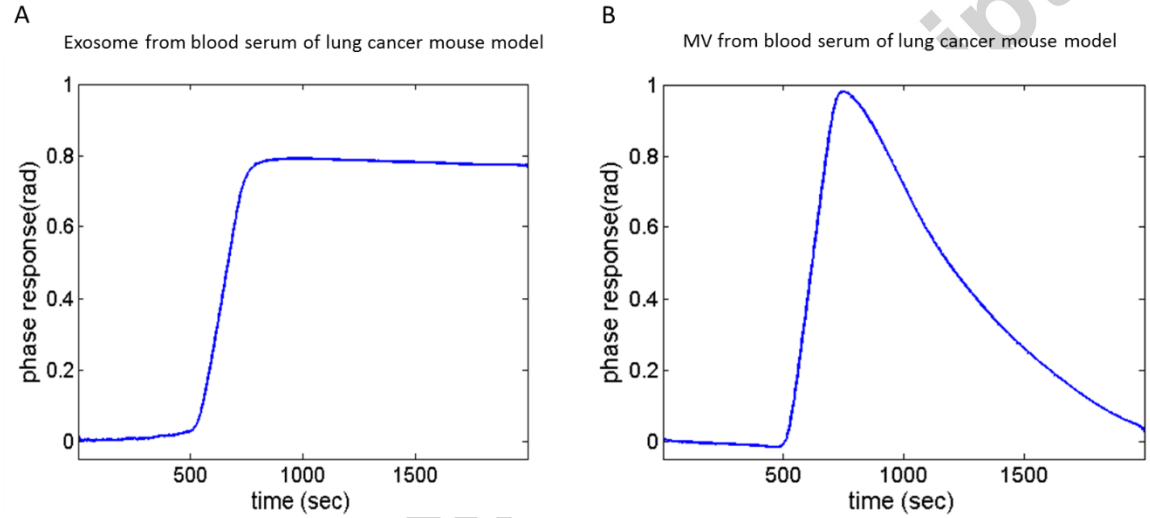

Fig 4 LSPR response to (A) exosomes and (B) MVs isolated from mouse blood serum: the phase response to exosomes from blood of tumor-bearing mice has low magnitude and shows high association compared to that of MVs.

3.5. AFM yields different force of separation for exosomes and MVs

To further confirm the observation (Figures 3 and 4) that binding affinity between MVs and SAM-AuNIs was less compared to that between exosomes and SAM-AuNIs, an AFM nanomechanical study was performed to analyze the force-separation pattern of exosomes and MVs separately with SAM-AuNIs. Figure 5 shows the typical approach/retract cycles taken between exosomes/MVs coated sensor tips and an AuNIs surface. The control experiment result is given in Figure 5(A) to show that bare tip has hardly any adhesion to AuNIs. According to Figure 5 (D-F), the mean adhesion force of exosome-AuNIs is significantly larger than that between MVs-AuNIs (Figure 5(G-I)). The mean interaction forces were concluded into the bar-chart as shown in Figure 5C. The adhesion forces of MVs were obviously lower than those of exosome-AuNIs. This has proven that in LSPR sensing test process, the buffer solution flowing force removed the MVs on AuNIs surface because of their weak interaction force. Moreover, the SH-SY5Y derived exosomes also exihibited larger interaction force with AuNIs than that of A-549 exosomes. It showed good agreement with the high LSPR response of SH-SY5Y derived exosomes as shown in figure 3A. It once

again proved that the interaction force between various cells' exosomes/MVs and AuNIs are different, and strongly supported the feasibility of our unfunctionalized AuNIs LSPR detection method.

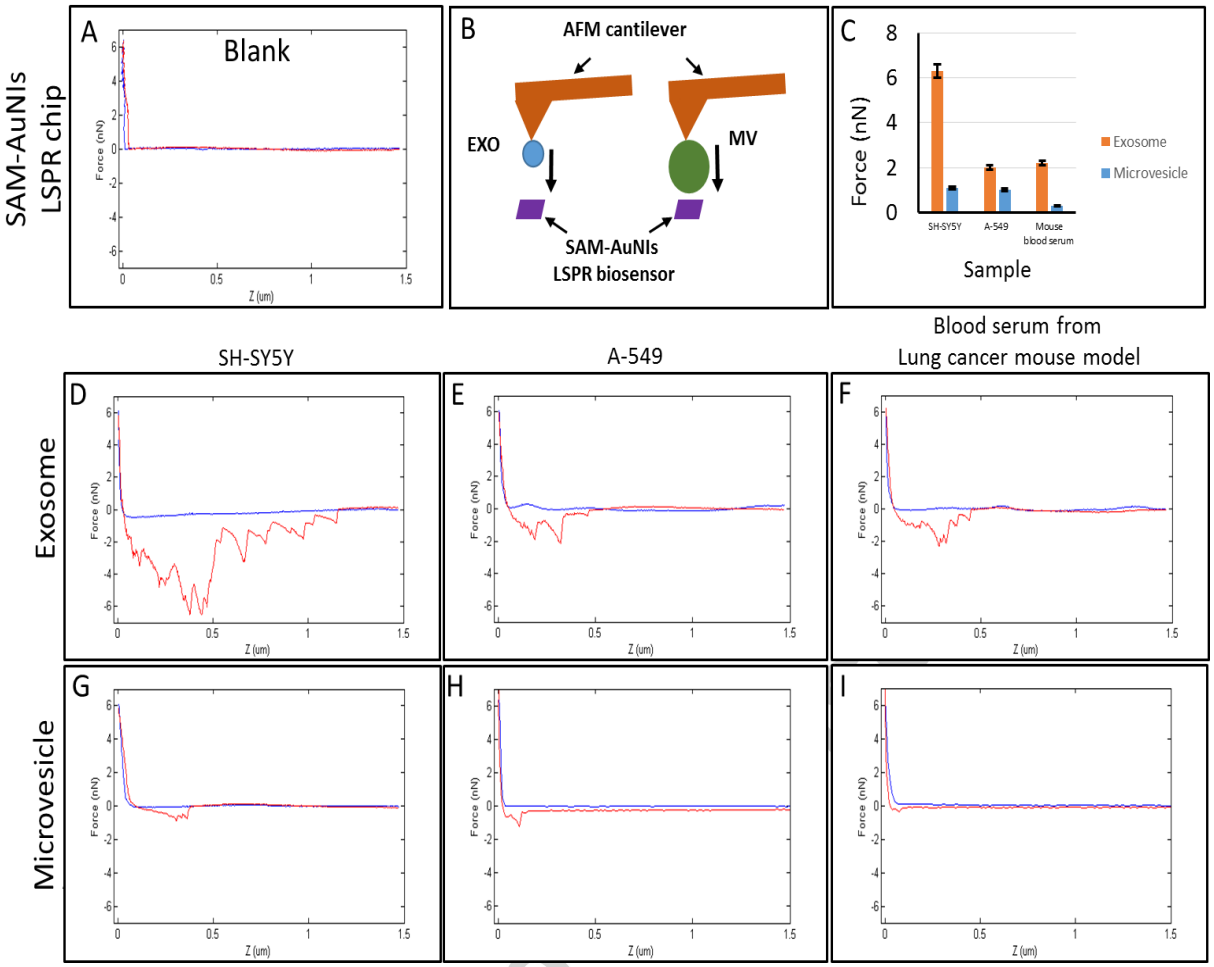

Fig 5 AFM nanomechanical study for interaction force study: (A) Control bare tip has hardly any adhesion to blank AuNIs, (B) representative image for the experimental setup for interaction force study, (C) bar graph representing the quantitative difference between force of interaction for exosomes and MVs with SAM-AuNIs LSPR chip. Interaction force study showed the mean adhesion force of exosome-AuNIs (D, E, and F) is significantly larger than that between MVs-AuNIs (G, H, and I).

4. Conclusions

Through this research with bare SAM-AuNIs for LSPR biosensing, we first found that the dissociation pattern for exosomes and MVs was significantly different, suggesting that the two types of vesicles had different binding affinity towards the SAM-AuNIs. Furthermore, force-separation analysis by AFM indicated the presence of higher interaction force between exosomes and AuNIs rather than between MVs and AuNIs. Finally, the zeta potential values of exosomes were more negative than that of MVs, indicating that exosomal membranes have a more aggregative property, tending towards being more attracted to bare gold nanoislands. Therefore, these findings not only clearly demonstrate the biophysical difference of the membrane of exosomes and MVs, but also provide great insight into the development of vesicle-specific biomarkers in disease progression via directly detecting differential membrane properties of tumor-derived exosomes and MVs by LSPR, AFM, and Malvern

Zetasizer Nano ZS. In conclusion, this work has strong potential to be extended to liquid biopsy applications in cancer diagnosis and prognosis.

Acknowledgements
This work was supported by the City University of Hong Kong start up grant (Grant no. 9610340 and 7200472). A. Thakur and G. Qiu are the recipients of the UGC fund for PhD at City University of Hong Kong. We are thankful to Mariana Abdulnoor (Summer exchange student in Dr. Lee's lab from University of Toronto, Canada) for her assistance in proof reading of the manuscript.

6. Conflict of Interest
The authors declare that they have no conflict of interest.

7. References
Almqvist, N., Lönnqvist, A., Hultkrantz, S., Rask, C. and Telemo, E., 2008. Immunology, 125(1), 21-27.
Amano, R., Takada, K., Tanaka, Y., Nakamura, Y., Kawai, G., Kozu, T. and Sakamoto, T., 2016. Biochem., 55(45), 6221-6229.
Beyer, C. and Pisetsky, D.S., 2010. Nat. Reviews Rheumatology, 6(1), 21-29.
Canoa, P., Rivadulla, M.L., Popplewell, J., van Oosten, R., Gómez, G. and Fall, Y., 2017. Anal. Bioanal. Chem., 1-12.
Chaput, N. and Théry, C., 2011. Seminars in immunopathol., 33(5), 419-440.
Florschütz, K., Schröter, A., Schmieder, S., Chen, W., Schweizer, P., Sonntag, F., Danz, N., Baronian, K. and Kunze, G., 2013. J. of virol. methods, 189(1), 80-86.
Gangoda, L., Boukouris, S., Liem, M., Kalra, H., & Mathivanan, S., 2015. Proteomics, 15(2-3), 260-271.
Gould, S.J., Booth, A.M. and Hildreth, J.E., 2003. PNAS, 100(19), 10592-10597.
György, B., Szabó, T.G., Pásztói, M., Pál, Z., Misják, P., Aradi, B., László, V., Pállinger, E., Pap, E., Kittel, A. and Nagy, G., 2011. Cell. & mol. life sci., 68(16), 2667-2688.
Huang, Y.Y., Hsu, H.Y. and Huang, C.J.C., 2007. Biosens. Bioelectron., 22(6), 980-985.
Im H, Shao H, Park Y I, et al., 2014. Nat. biotechnol., 32(5): 490-495.
Jayachandran, M., Miller, V.M., Heit, J.A. and Owen, W.G., 2012. J. immunol. methods, 375(1), 207-214.
Kesimer, M., Scull, M., Brighton, B., DeMaria, G., Burns, K., O'Neal, W., Pickles, R.J. and Sheehan, J.K., 2009. FASEB., 23(6), 1858-1868.
Li, M., Zeringer, E., Barta, T., Schageman, J., Cheng, A. and Vlassov, A.V., 2014. Phil. Trans. R. Soc. B, 369(1652), 20130502.
Lin, J., Li, J., Huang, B., Liu, J., Chen, X., Chen, X.M., Xu, Y.M., Huang, L.F. and Wang, X.Z., 2015. The Sci. World J.
Marzesco, A.M., Janich, P., Wilsch-Bräuninger, M., Dubreuil, V., Langenfeld, K., Corbeil, D. and Huttner, W.B., 2005. J. cell sci., 118(13), 2849-2858.
Mazzeo, C., Cañas, J.A., Zafra, M.P., Marco, A.R., Fernández-Nieto, M., Sanz, V., Mittelbrunn, M., Izquierdo, M., Baixaulli, F., Sastre, J., and del Pozo, V., 2015. J. of Allergy and Clin. Immunol., 135(6), 1603-1613.

Morel, O., Jesel, L., Freyssinet, J.M. and Toti, F., 2011. Arterioscler., thromb., vasc. boil., 31(1), 15-26.

Ng, S.P., Qiu, G., Ding, N., Lu, X. and Wu, C.M.L., 2016. Biosens. Bioelectron., 89 (2017), 468-476.

Pocsfalvi, G., Stanly, C., Vilasi, A., Fiume, I., Capasso, G., Turiák, L., Buzas, E.I. and Vékey, K., 2016. Mass spectrum. Rev., 35(1), 3-21.

Qiu, G., Ng, S.P. and Wu, C.M.L., 2015. Optics letters, 40(9), 1924-1927.

Rood, I.M., Deegens, J.K., Merchant, M.L., Tamboer, W.P., Wilkey, D.W., Wetzels, J.F. and Klein, J.B., 2010. Kidney international, 78(8), 810-816.

Sharma, S., Rasool, H. I., Palanisamy, V., Mathisen, C., Schmidt, M., Wong, D. T., & Gimzewski, J. K., 2010. Acs Nano, 4(4), 1921-1926.

Sikarwar, B., Singh, V.V., Sharma, P.K., Kumar, A., Thavaselvam, D., Boopathi, M., Singh, B. and Jaiswal, Y.K., 2017. Biosens. Bioelectron., 87, 964-969.

Soler, M., Estevez, M.C., de Lourdes Moreno, M., Cebolla, A. and Lechuga, L.M., 2016. Biosens. Bioelectron., 79, 158-164.

Tamada, K., Nakamura, F., Ito, M., Li, X. and Baba, A., 2007. Plasmonics, 2(4), 185-191.

Théry, C., Amigorena, S., Raposo, G. and Clayton, A., 2006. Curr. Protoc. cell biol., Chapter 3:Unit 3.22.

Théry, C., Ostrowski, M. and Segura, E., 2009. Nature Reviews Immunology, 9(8), 581-593.

van der Pol, E., Böing, A.N., Harrison, P., Sturk, A. and Nieuwland, R., 2012. Pharmacol. Rev., 64(3), 676-705.

Xu, R., Greening, D.W., Rai, A., Ji, H. and Simpson, R.J., 2015. Methods, 87, 11-25.

Yáñez-Mó, M., Siljander, P.R.M., Andreu, Z., Zavec, A.B., Borràs, F.E., Buzas, E.I., Buzas, K., Casal, E., Cappello, F., Carvalho, J. and Colás, E., 2015. J. of extracell. Ves., 4.

Yuana, Y., Oosterkamp, T.H., Bahatyrova, S., Ashcroft, B., Garcia Rodriguez, P., Bertina, R.M. and Osanto, S., 2010. J. thromb. & haemost., 8(2), 315-323.

Highligths

- A time and cost effective method for directly detecting exosomes and microvesicles with a concentration-dependent manner.
- Exosomes and microvesicles can be differentiated clearly by an antibody-unfunctionalized SAM-AuNIs LSPR biosensor.
- A significant difference exists in the biophysical interaction of exosomes and microvesicles with gold nanoislands.